Nonlinear analysis of the pharmacological conversion of sustained atrial fibrillation in conscious goats by the class Ic drug cibenzoline

Bart P. T. Hoekstra
Department of Physiology, University of Leiden, P.O. Box 9604, 2300 RC Leiden, The Netherlands

Cees G. H. Diks
Institute of Mathematics and Statistics, University of Kent at Canterbury, Canterbury, Kent CT2 7NF, United Kingdom

Maurits A. Allessie
Department of Physiology, Cardiovascular Research Institute Maastricht, Maastricht University, P.O. Box 616, 6200 MD Maastricht, The Netherlands

Jacob DeGoede
Department of Physiology, University of Leiden, P.O. Box 9604, 2300 RC Leiden, The Netherlands

(Received 14 January 1997; accepted for publication 30 April 1997)

Methods from nonlinear dynamics were applied to test the hypothesis that the dynamics of sustained atrial fibrillation (AF) is modified by the class Ic drug cibenzoline during pharmacological conversion. The experiments were performed in conscious goats in which sustained AF was induced by continuous maintenance of AF via programmed electrical stimulation. Data were collected from electrophysiological experiments in five goats to terminate sustained AF by continuous infusion of cibenzoline. Sets of five unipolar epicardial electrograms of one minute duration were recorded from the left and right atrial free wall during sustained AF (control), and at three episodes during infusion of cibenzoline, when the mean AF interval had been prolonged to 25%, 50% and 85% with respect to control. Ventricular far-field potentials were removed from atrial electrograms by a coherent averaging procedure. Using the Grassberger-Procaccia method, the dynamics of the local atrial electrograms was investigated by estimating the (coarse-grained) correlation dimension and correlation entropy from the correlation integral. The results were related to a recently proposed classification (types I–III) of AF based on the degree of complexity of atrial activation patterns. The coarse-grained correlation dimension D_{cg} and entropy K_{cg} indicated that sustained AF corresponded to type II. During drug administration the coarse-grained parameters were not significantly different from control. Scaling regions in the correlation integral were observed after infusion of cibenzoline (3 out of 5 goats) suggesting that the drug introduced low-dimensional features (type I) in the dynamics of AF (correlation dimension D ranging from 2.8 to 4.4 and correlation entropy K from 1.6 to 6.2 nats/s). Sinus rhythm recorded shortly after cardioversion was very regular ($D<2$ and $K<3$ nats/s). The hypothesis that the electrograms during AF and sinus rhythm were generated by a static transformation of a linear Gaussian random process was rejected using a test for time reversibility. The nonlinear analysis revealed that cibenzoline does not significantly alter the dynamics of sustained AF during pharmacological conversion other than a slowing down of the atrial activation and a somewhat increasing global organization of the atrial activation pattern. The sudden change in the dynamical behavior at cardioversion suggests a mechanism that is reminiscent of a bifurcation. © *1997 American Institute of Physics.* [S1054-1500(97)00703-9]

Currently, pharmacological treatment is the main therapeutic strategy in the control of atrial fibrillation (AF). However, the anti-arrhythmic mechanisms are still not understood in detail and pro-arrhythmic side effects during drug therapy have been observed. In this study, we investigated the anti-fibrillatory properties of the class Ic agent cibenzoline in instrumented conscious goats in which sustained AF had been electrically induced. We tested the hypothesis that this drug alters the dynamics of sustained AF using methods from nonlinear time series analysis. Nonlinear ''complexity parameters'' like the coarse-grained correlation dimension and entropy were estimated from epicardial atrial electrograms recorded during electrophysiological experiments to terminate AF. The results were related to a recently proposed classification (types I–III) of AF based on the degree of complexity of atrial activation patterns visualized from epicardial mapping. The nonlinear parameters indicated that sustained AF is of an intermediate level of complexity (type II). During administration of cibenzoline the dynamical complexity remained close to control, although in some goats scaling regions were identified in the correlation integral, indicating increased global organization (type I) in the atrial activation patterns. Although cibenzoline affects electrophysiological characteristics like activation interval and conduction velocity, it is concluded from the nonlinear analysis that this drug induced no marked modifications in the dynamics of sustained AF

other than a slowing down of the electrical activation and a somewhat increased global organization of atrial activation patterns. This suggests that, to a first approximation, the dynamics of sustained AF and of the pharmacologically modified substrate of AF are orbitally equivalent. Sinus rhythm recorded shortly after cardioversion of AF was very regular and resembled a noisy limit cycle. Our findings suggest that pharmacological conversion of sustained AF to sinus rhythm by cibenzoline is mediated through a bifurcation of the dynamics.

I. INTRODUCTION

Atrial fibrillation (AF) is clinically the most common cardiac arrhythmia, with an increasing prevalence up to 2%–4% in the population over 60 years of age. It is characterized by rapid, uncoordinated contractions of the atria, a diminished ventricular ejection fraction and a fast, irregular heart rate. Restoring and maintaining the normal sinus rhythm via electrical direct current cardioversion is in many cases effective in patients with a recent onset of atrial fibrillation (paroxysmal AF). In patients with chronic atrial fibrillation, however, sinus rhythm is often not maintained after electrical defibrillation and active drug therapy is needed to prevent recurrent induction of AF. Nowadays, pharmacological intervention remains the major therapeutic strategy to control AF.[1] It is known that the success to terminate AF by anti-arrhythmic drugs strongly depends on the duration of the arrhythmia. Due to the progressive nature of AF, it may not be possible to restore and maintain sinus rhythm when AF has persisted over a longer period of time despite prophylactic drug therapy. In that case the control of the ventricular rate together with anticoagulation to prevent thromboembolic events associated with this rhythm disturbance may become the main therapeutic goal.

Despite the success of pharmacological treatment, it has become increasingly clear that anti-arrhythmic drugs also display potentially dangerous proarrhythmic effects. For instance, the results of the Cardiac Arrhythmia Suppression Trial[2] (CAST) have pointed out that the anti-arrhythmic action of so-called class Ic drugs is not without risk, especially for patients with a history of heart disease. Observations like these have recently raised a renewed interest to understand the mechanisms of drug action in detail (see, e.g., Refs. 3–7).

The recently introduced drug cibenzoline is, according to the Vaughan Williams classification,[8] a class Ic drug whose main action is a blockade of sodium channels during depolarization of the transmembrane potential resulting in depressed excitability and a decreased conduction velocity. It also shows additional class III and IV effects prolonging the repolarization phase of the action potential. However, it is not clear whether this classification helps to understand the effectiveness of pharmacological conversion of cardiac arrhythmias. It is conceivable that arrhythmias with different dynamical properties may be converted by the same type of drug, while on the other hand the same type of arrhythmogenic dynamics may be converted by different types of drugs. Therefore, it is important to understand drug action not only in terms of the effects on electrophysiological parameters like local activation interval, conduction velocity and refractory period, but also in terms of the induced changes in the underlying ''type'' of dynamics of the arrhythmia.

The mathematical theory of dynamical systems has led to new methods to characterize the underlying dynamics generating experimentally observed time series. A number of books[9,10] and review articles[11,12] give an excellent introduction to this subject. These methods, collectively called nonlinear time series analysis, have only recently been introduced in the field of cardiology and have been applied for instance to cardiac time series of sinus rhythm, ventricular tachycardia and fibrillation.[13–19] We have previously applied nonlinear analysis to characterize and classify electrograms of electrically induced acute atrial fibrillation in man.[20]

In the present study atrial electrograms were characterized by nonlinear analysis to test the hypothesis that cibenzoline, which is known to exert strong effects on the electrophysiological substrate of AF,[21] alters the dynamics of sustained AF during pharmacological conversion. Epicardial atrial electrograms were recorded in instrumented conscious goats in which sustained AF was induced by a fibrillation pacemaker.[22] Whereas the action of anti-arrhythmic agents is usually tested during sinus rhythm or slow pacing, this recently developed goat model of sustained AF offers the possibility to directly test the anti-fibrillatory effect of drugs in a setting in which AF has become permanent in an otherwise normal heart.

II. METHODS

A. Data acquisition

Five goats were instrumented with a teflon felt strip (10 cm $\times$ 1.2 cm) containing 23 electrodes (silver, diameter 1.5 mm), positioned along Bachmann's bundle and fixed to both atrial appendages. The distance between the electrodes was 6–10 mm. Two other felt plaques (3.5 cm $\times$ 2.5 cm), each containing 30 electrodes, were sutured to the left and right atrial lateral wall (electrode distance 4.0–5.7 mm). A felt strip containing four electrodes was sutured to the left ventricular epicardium. All leads were tunneled subcutaneously to the neck and exteriorized by three 30-pin connectors (Lemosa®, outer diameter 10 mm). Three silver plates (diameter 25 mm) were left subcutaneously to serve as grounding and indifferent electrodes. Figure 1 shows a schematic drawing of the implanted atrial electrodes.

About 3 weeks after implantation, the goats were connected to an external automatic fibrillator. This device repetitively induced AF by burst pacing as soon as sinus rhythm was detected in one of the atrial electrograms. In this way AF was maintained during 24 hours a day, 7 days a week. Continuous maintenance of AF resulted in sustained atrial fibrillation (duration longer than 24 hours) in a time varying from a few days to 3 weeks. The electrode configuration was used to measure electrophysiological parameters like local fibril-

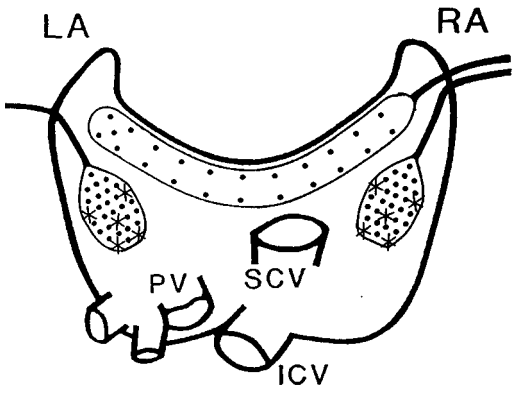

FIG. 1. Configuration of the implanted epicardial atrial electrodes. A teflon felt strip containing 23 electrodes was positioned along Bachmann's bundle (electrode distance 6–10 mm). Two other felt strips, each containing 30 electrodes, were sutured to the left and right atrial lateral walls (electrode distance 4.0–5.7 mm). Electrodes indicated by asterisks were chosen for analysis. LA, left atrium; RA, right atrium; PV, pulmonary veins; SCV, superior caval vein; ICV, inferior caval vein.

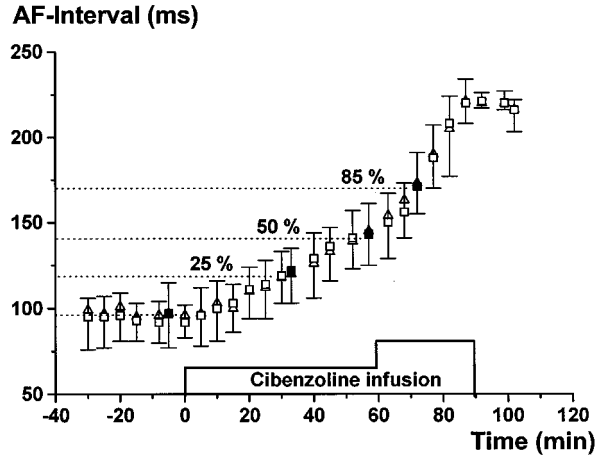

FIG. 2. Progressive prolongation of atrial fibrillation (AF) intervals during the continuous infusion of cibenzoline. During the first 60 minutes cibenzoline was infused at a rate of 0.1 $mg \cdot kg^{-1} \cdot min^{-1}$, followed by 30 minutes at 0.2 $mg \cdot kg^{-1} \cdot min^{-1}$. Cibenzoline gradually increased the mean AF interval from 92 to 206 ms. After 119 minutes AF converted to sinus rhythm (goat no. 4). Electrograms of AF were recorded during control and when the mean AF interval had been prolonged with 25%, 50% and 85% (indicated by dotted lines and filled symbols). Intervals (mean $\pm$ sd) were measured from a bipolar lead at the left (triangles) and right (squares) atrial lateral walls.

lation interval, intra atrial conduction velocity and the effective refractory period during the development of sustained AF in instrumented conscious goats. For a detailed description of the conscious goat model of sustained atrial fibrillation see Wijffels *et al.*[22]

B. Data selection

We selected 5 of the 30 electrograms recorded at the lateral wall of both the left and right atrium during electrophysiological experiments to study the anti-fibrillatory action of cibenzoline. Unipolar electrograms of 1 minute duration were recorded (gain 300 to 600), bandpass filtered (1 to 500 Hz), multiplexed (sampling rate 1 kHz) and AD converted (resolution 8 bits), from electrode positions indicated by asterisks in figure 1. If electrograms contained artifacts or showed a low signal to noise ratio, a neighboring electrode was chosen. A ventricular reference electrogram was recorded as well.

The class Ic drug cibenzoline (Cipralan®, Searle, Belgium) was administered by intravenous infusion at a rate of 0.1 $mg \cdot kg^{-1} \cdot min^{-1}$. In figure 2 an example of the effects of cibenzoline on the mean AF interval is given (goat no. 4). Starting 30 minutes before the onset of infusion of cibenzoline, mean AF intervals were determined every 5 minutes both at the left (triangles) and the right atrium (squares). Cibenzoline caused a dose dependent increase in the mean AF interval. In two goats (nos. 2 and 4) after 60 minutes the infusion rate was increased to 0.2 $mg \cdot kg^{-1} \cdot min^{-1}$. After 90 minutes infusion of cibenzoline was stopped.

Figure 2 illustrates how AF episodes were selected for nonlinear analysis: AF electrograms were selected both during sustained AF (control), and when the AF interval had been prolonged to 25, 50 and 85 percent compared to control. We refer to these episodes as CIB25, CIB50 and CIB85. The mean total duration of atrial fibrillation was 50 $\pm$ 50 days, whereas the episode of sustained AF that was converted by cibenzoline had lasted 36 $\pm$ 46 days. In table I for all goats the effects of cibenzoline on the AF cycle length are given. In one experiment (goat no. 2) AF did not convert. After AF was terminated by cibenzoline, a segment of sinus rhythm was selected in three goats.

C. Coherent averaging of the ventricular response

During AF far-field potentials originating from the electrical activity of the ventricles are a confounding element in the analysis of local electrical activity of the atria. A coherent averaging procedure was applied to remove the ventricular deflections from the atrial fibrillation electrograms.

Figure 3 illustrates this averaging procedure in a right atrial electrogram (RA). A left ventricular electrogram (LV) was used as time reference for the ventricular far-field potential. A template of the ventricular far-field potential was obtained by averaging all time windows of the RA electrogram around the *R*-wave detected in the LV electrogram. Since during AF the *R*-wave is completely dissociated from the atrial activity, the atrial signals are averaged out, and the resulting template solely represents the ventricular far-field potential picked up by the atrial electrode. By subtracting this template from the corresponding time windows in the RA electrogram, the ventricular far-field potentials are removed. Further details of the calculation of the template are given in the Appendix.

The coherent averaging procedure used offers a simple and relatively straightforward procedure to remove ventricular far-field contributions in atrial electrograms. We did not construct bipolar leads to eliminate nonlocal deflections, because the interelectrode distance (4.0–5.7 mm) was too large for an appropriate local measurement of atrial activation.

TABLE I. Effects of cibenzoline on cycle length of atrial fibrillation. AF indicates atrial fibrillation; SAF, sustained atrial fibrillation (longer than 24 hours); SR, sinus rhythm; LA, left atrium; RA, right atrium; CIB25, CIB50, CIB85, atrial fibrillation during infusion of cibenzoline when the AF interval had been prolonged to 25%, 50% and 85%, respectively, compared to control. Intervals are denoted as mean and were measured from a single atrial bipolar electrogram. The relative prolongation of the AF interval is indicated between parentheses. An asterisk denotes intervals which were determined from the last minute before the termination of AF.

			Interval of atrial fibrillation												
			SAF		CIB25		CIB50		CIB85		Stop of AF*				
Goat no.	Weight kg	Duration of SAF days	LA ms	RA ms	LA ms (%)	RA ms (%)	LA ms (%)	RA ms (%)	LA ms (%)	RA ms (%)	LA ms (%)	RA ms (%)	Stop of AF min	Total dose of cibenzoline mg/kg	Interval of SR ms
1	50	4	97	104	110 (13)	127 (22)	137 (41)	161 (55)	186 (92)	195 (88)	219 (126)	220 (112)	51	5.1	611
2	45	14	96	96	113 (18)	118 (23)	143 (49)	144 (50)	183 (91)	178 (85)	—	—	—	10.6	—
3	58	115	107	102	139 (30)	136 (33)	156 (46)	155 (52)	180 (68)	177 (73)	180 (68)	177 (74)	60	6.0	531
4	40	37	96	92	120 (25)	122 (33)	145 (51)	143 (55)	173 (80)	171 (86)	209 (118)	206 (124)	119	12.0	524
5	81	8	108	97	124 (15)	112 (16)	162 (50)	145 (50)	197 (82)	178 (84)	197 (82)	178 (84)	47	3.9	452
Mean	55	36	101	98	121 (20)	123 (25)	149 (47)	150 (52)	184 (83)	180 (83)	201 (99)	195 (99)	69	7.5	530
SD	16	46	6	5	11 (7)	9 (7)	10 (4)	8 (3)	9 (10)	9 (6)	17 (28)	21 (23)	34	3.6	65
Mean			100		122 (23)		149 (50)		182 (83)		198 (99)				
SD			5		10 (7)		9 (4)		9 (8)		18 (24)				

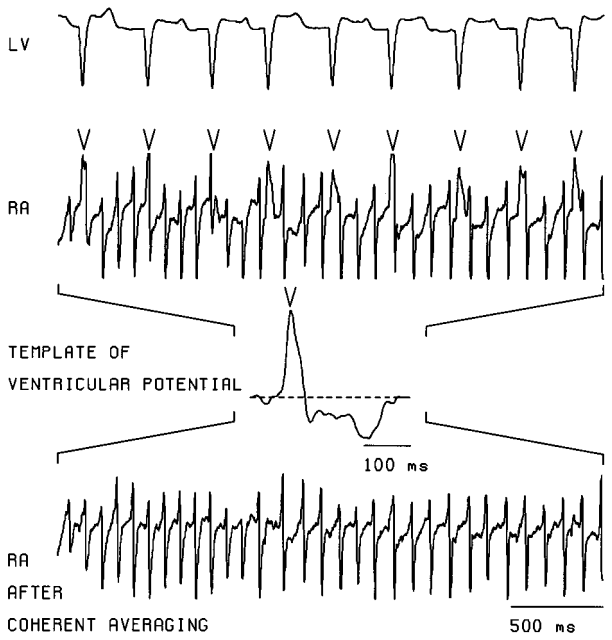

FIG. 3. Coherent averaging procedure to remove far-field ventricular potentials from unipolar epicardial atrial electrograms during atrial fibrillation (AF). A right atrial electrogram (RA) is shown during sustained AF (goat no. 2). A template of the ventricular far-field potential was obtained by averaging all time windows of the RA electrogram around the detected *R*-wave (marked by V) in the LV electrogram. The far-field ventricular potentials were removed by subtracting this template from the corresponding time windows in the RA electrogram.

D. Reconstructing dynamics

During an experiment, information about the state of the system is obtained via the measurement of a time series $\{v(i)\}_{i=1}^{L}$ consisting of L values at sample times $i\Delta t$, where Δt is the sample interval. Nonlinear analysis starts with reconstructing the dynamics of the system from the measured time series. To this end delay vectors $\vec{x}(i)$ are constructed in a so-called state space or phase space using lagged values of the time series as vector components, viz.

$$\vec{x}(i)=(v(i),v(i+l),v(i+2l),\ldots,v(i+(m-1)l)), \tag{1}$$

where l is the embedding delay and m is the embedding dimension of the reconstruction. According to Takens' reconstruction theorem[23] the dynamical characteristics of the reconstructed system are the same as those of the real (physiological) system when m is large enough. For a stationary, infinitely long and noise-free time series the embedding delay can be chosen almost arbitrarily. However, for a finite recorded electrogram which is contaminated with an unknown amount of noise, the delay l has to be selected properly. We chose a value for l which is equal to the lag corresponding to the first minimum of the mutual information function.[24] Before entering the calculations (after coherent averaging of the ventricular response), electrograms were sampled down to 30000 points, containing about 300

(CIB85) to 600 (sustained AF) fibrillation intervals. Thus after data reduction, electrograms contained about 50 to 100 samples per fibrillation interval.

Although the original time series may appear erratic, a hidden structure in the dynamics can be revealed by considering the time series $\vec{x}(i)$ obtained by the process of reconstruction. In practice this is often done by visual inspection of a phase plot. In such a plot, the first two components of a delay vector are plotted against each other for consecutive time indices i, constituting a two-dimensional projection of the trajectory in the reconstructed phase space.

E. Correlation dimension and entropy

The correlation integral was introduced[25,26] to characterize complex dynamical behavior generated by simple nonlinear systems. Grassberger and Procaccia (GP) proposed a now standard method to estimate the correlation integral from observed time series. We used a modified version of the GP method,[27,28] the details of which are given in the Appendix.

To identify low-dimensional dynamics from a time series, one first looks for a linear part, the so-called ''scaling region,'' in a double logarithmic plot of the correlation integral $C_m(r)$ as a function of distance r in reconstructed phase space of embedding dimension m. The correlation dimension D_m is then estimated as the slope of the correlation integral within the scaling region. The correlation entropy K_m can be estimated from the distance between the correlation integrals within the scaling region as m is increased in a double logarithmic plot of $C_m(r)$ versus r and is expressed in units nats/s using the natural logarithm. In case D_m and K_m saturate as a function of m, these values are taken as estimates of the correlation dimension and correlation entropy, respectively. The correlation dimension is considered as a measure for the number of coupled modes which describe the observed behavior. The correlation entropy is associated with the unpredictability of the dynamics. When the entropy increases, the future behavior of the system can be predicted with less accuracy.

It is known that the correlation dimension may slowly converge to its asymptotic value due to a lack of data.[29] Therefore, the embedding dimensions were taken large and in electrograms of AF, D_m and K_m were averaged over embedding dimensions 14 to 18 to reduce the variability. During sinus rhythm the results were averaged over embedding dimensions 18 to 22. For the range of embedding dimensions and delays used, the embedding window $T=(m-1)l\Delta t$ contained several characteristic cycles of the epicardial electrograms: about 4 to 8 fibrillation intervals and 1 to 2 intervals of sinus rhythm. It is our experience that, for the given type of data, the embedding window has to contain several characteristic cycles to obtain convergence of the correlation entropy.[30]

As there currently exist no objective criteria to identify a scaling region, curves of coarse-grained correlation dimension and entropy were also determined to guide the eye in the selection of a scaling region. The interval of distances where these curves tended to level off with increasing embedding dimension was selected as a scaling region. In order not to be rejected, a selected scaling region had to extend over at least one binade. Furthermore, the estimated correlation dimension had to be smaller than 5, otherwise it was not tabulated and the scaling region was not accepted.

When there is no clear indication of a scaling region, the correlation integral is still useful to characterize the dynamics. The correlation integral is then estimated at a fixed embedding dimension m and finite resolution r in reconstructed phase space. In this way coarse-grained ''complexity parameters'' can be defined which quantify the underlying dynamics.[31–34] The coarse-grained correlation dimension $D_m(r)$ is defined as the local slope of the correlation integral in a double logarithmic plot of $C_m(r)$ versus r. In such a plot, the coarse-grained correlation entropy $K_m(r)$ is defined by the decrement of the correlation integrals at distance r when embedding dimension m is increased. We evaluated the coarse-grained correlation dimension (D_{cg}) and entropy (K_{cg}) at embedding dimension 10 for AF and 20 for sinus rhythm, at a distance r_{cg} equal to the standard deviation of the time series divided by its peak-to-peak value. We refer to the Appendix for details of the implementation to estimate the correlation dimension and correlation entropy and the corresponding coarse-grained quantities.

F. Testing for time reversibility

It is by now well recognized that the methods from nonlinear dynamics should be applied prudently and the results should be interpreted with care. For instance, low-dimensional behavior may be readily identified from time series generated by a (linear) stochastic process. To investigate whether the electrograms were generated by a linear Gaussian random process, we applied a recently proposed method[35] which tests for the property of time reversibility in a time series.

A time series is called (time) reversible if its statistical properties are invariant under the reversal of time direction. This means that the time series ''looks the same'' read forward or backward in time. Otherwise the time series is said to be (time) irreversible. If reversibility can be ruled out, the hypothesis can be rejected that the time series is a realization of a static transformation of a linear Gaussian random process.

To be more specific, consider a ''time reversed'' delay vector constructed by inverting the order of the vector components in equation (1). If a time series is reversible, the distribution of the time reversed delay vectors and the distribution of original delay vectors are identical. For instance, in a two-dimensional phase plot (v_i, v_{i+l}), reversibility may be examined by interchanging the two components of the delay vectors. This is equal to mirroring the plot in the main diagonal. If the plot is not symmetric with respect to this operation (i.e., with respect to time reversal), it can be concluded that the time series is irreversible.

Reversibility can be rejected at a significance level 0.05 when the test statistic S gets larger than three. This criterion was used in the calculations to reject reversibility in the mea-

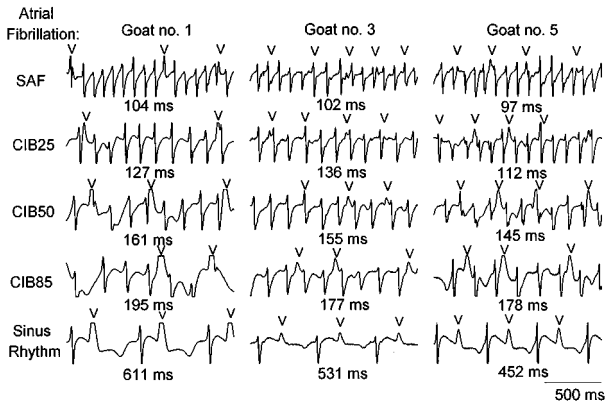

FIG. 4. Right atrial electrograms of sustained atrial fibrillation (SAF) and of atrial fibrillation during infusion of cibenzoline in three goats. Electrograms are shown when the mean fibrillation interval had been prolonged to 25%, 50% and 85% with respect to control (indicated by CIB25, CIB50 and CIB85, respectively). Electrograms of sinus rhythm were recorded shortly after cardioversion. Numbers indicate mean intervals during atrial fibrillation and sinus rhythm. V, ventricular complex.

sured electrograms. Furthermore, the effects of drug loading were monitored by estimating the quantity Q, which is a measure for the distance between the delay vector distributions of the original and time reversed electrograms. The larger Q, the more the observed time series deviates from its time reversed copy. The test, its implementation and the choice of the parameters involved are described in more detail in the Appendix.

G. Statistical analysis

Two-way analysis of variance with a fixed model was applied (SAS software package, SAS Institute Inc., USA) to test for differences in coarse-grained correlation dimension, entropy and the reversibility statistic Q during AF, with goats and drug dose as factors. Each cell contained the mean value resulting from the analysis of five electrograms recorded at the left or right atrial lateral wall (indicated by asterisks, figure 1). Bonferroni's t test was used to compare the estimated values at different dose of cibenzoline. A probability value $p<0.05$ was considered to be statistically significant.

III. RESULTS

A. Electrograms and phase plots

Figure 4 shows right atrial electrograms recorded from three goats during infusion of cibenzoline. Most of the time, electrograms showed discrete complexes without a high degree of fragmentation in the waveform morphology. At an increasing dose of cibenzoline the rate of AF gradually decreased, and atrial activation complexes widened in the course of the experiment. The mean AF interval in the five goats before the start of infusion of cibenzoline was 100 ± 5 ms (table I). In the last minute before conversion to sinus rhythm the mean AF interval had increased to 198 ± 18 ms. In figure 4 the occurrence of ventricular activation is indicated in the atrial electrograms. Note that ventricular deflections are clearly visible in the local atrial recordings at an increasing dose of cibenzoline. Apart from the effects on the AF cycle length and electrogram configuration, cibenzoline was also effective in converting sustained AF (4 out of 5 goats, 80%). Sinus rhythm after cardioversion of AF was very regular, the standard deviation of the beat-to-beat cycle length being less than 10 ms.

We studied the effects of this powerful anti-arrhythmic action on the dynamics of sustained AF by performing a nonlinear analysis of atrial electrograms during infusion of cibenzoline. In figure 5, we give a representative example and in the following we go through the various steps involved. The ventricular far-field potentials were first removed from the AF electograms by the method of coherent averaging. In this example (goat no. 3), the AF interval increased from 102 ms during control to 177 ms during the last minute before conversion to sinus rhythm. First, phase plots were constructed to give an impression of the underlying dynamics. During AF these plots displayed cross-like patterns, which reflect the presence of discrete activation complexes. Note that the excursions into the upper part of the phase plot are absent during administration of cibenzoline. The trajectory of sinus rhythm resembled a limit cycle (closed loop), thus illustrating the periodicity in the recorded electrogram. Values of the embedding delays of the analyzed electrograms during AF and sinus rhythm were in the range of 35 to 65 ms.

B. Identifying low-dimensional features

We next examined all electrograms for the existence of a scaling region in the correlation integrals to identify low-dimensional features in the dynamics. In figure 5, correlation integrals are shown for embedding dimensions 2 (top curve) to 20 (bottom curve), in increments of 2. In the correlation integrals of sustained AF no apparent scaling regions were found. However, during infusion of cibenzoline scaling regions (indicated between dashed lines) were identified in the range [0.14;0.37] of distances in phase space. Correlation dimension D was 3.3 ± 0.2 (CIB25), 3.2 ± 0.2 (CIB50) and 3.8 ± 0.2 (CIB85), respectively. Correlation entropy K progressively decreased from 5.0 ± 0.3 nats/s (CIB25) to 3.8 ± 0.1 nats/s (CIB85). During sinus rhythm a scaling region was present at distances [0.07;0.16], and the dynamics were characterized with $D = 1.3 \pm 0.1$ and $K = 1.0 \pm 0.2$ nats/s. At the bottom of figure 5 curves of correlation dimension D_m and correlation entropy K_m are shown as a function of increasing embedding dimension m. Note the oscillations which are present in the curves of K_m as a function of embedding dimension m during control and infusion of cibenzoline. These oscillations occurred using our choice for the reconstruction parameters and were characteristic for the correlation entropy estimated from AF electrograms containing a strong periodic component. The period p of the oscillations observed in the curves K_m corresponds to a time interval $\Delta T = pl\Delta t$ (where l is the embedding delay and Δt the sample interval) which was about equal to the mean AF cycle length of the electrograms analyzed. In the curves K_m

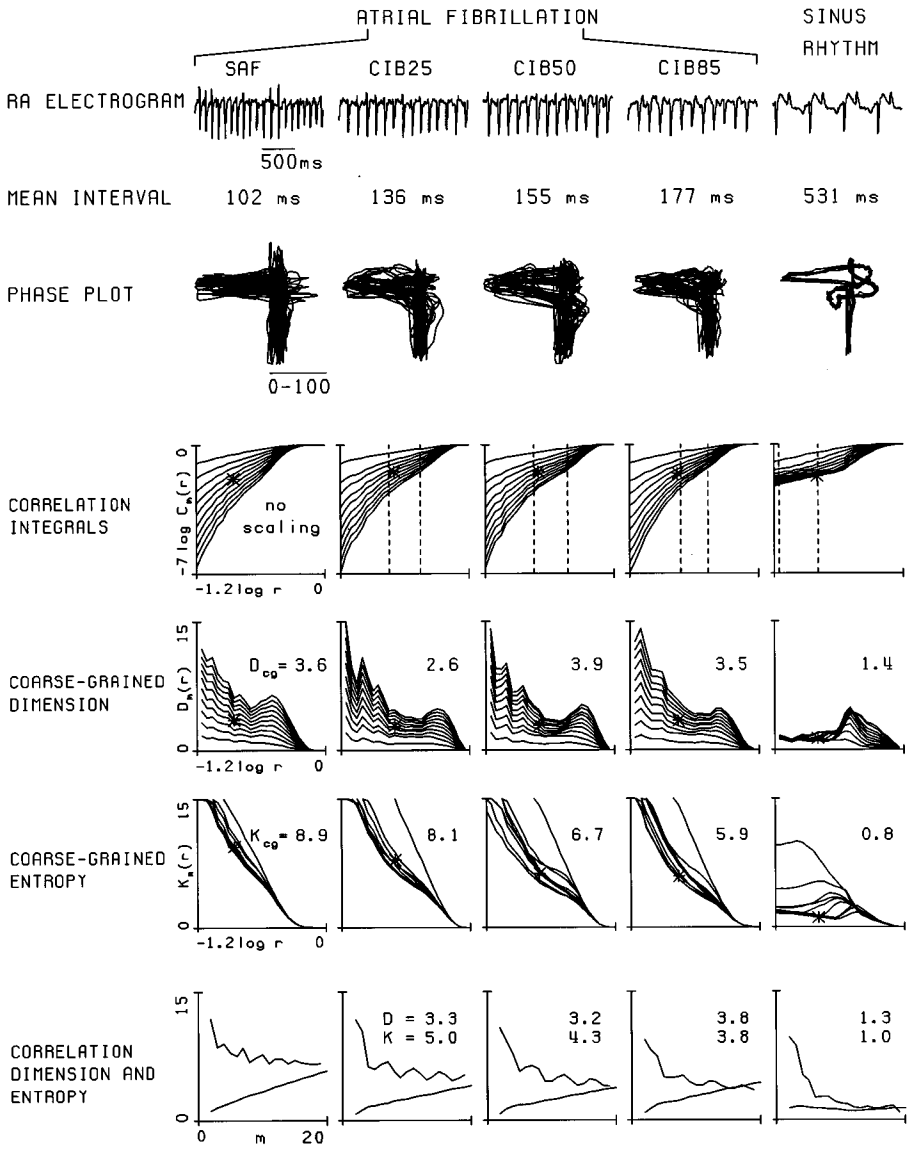

FIG. 5. Right atrial electrograms (RA) during sustained atrial fibrillation (SAF) and during infusion of cibenzoline (CIB25, CIB50, CIB85). Most of the time the electrograms during atrial fibrillation (AF) showed discrete activation complexes (goat no. 3). During infusion of cibenzoline the mean AF interval increased from 102 ms to 177 ms. After 60 minutes AF converted into sinus rhythm with an interval of 531 ms. Phase plots are constructed using embedding delays 36, 32, 34, 36 and 56 ms (left to right). During AF the trajectory generated a cross-like structure in reconstructed phase space. The phase plot of sinus rhythm resembled a noisy limit cycle. Correlation integrals $C_m(r)$ are shown in a double logarithmic plot (base 10) as a function of distance r in reconstructed phase space. Embedding dimension m ranged from 2 (top curves) to 20 (bottom curves), in increments of 2. Curves of $D_m(r)$ and $K_m(r)$ were derived from the correlation integrals and coarse-grained correlation dimension D_{cg} and entropy K_{cg} were estimated at embedding dimension 10 (AF) and 20 (sinus rhythm) at a distance equal to the standard deviation of the electrogram divided by its peak-to-peak value (indicated by asterisks). Scaling regions were identified (between dashed lines) in the AF correlation integrals at distances in the range [0.14–0.37]. During sinus rhythm a scaling region was found at distances [0.07–0.16]. *Bottom:* Correlation dimension D_m (lower curves) and correlation entropy K_m (upper curves, units nats/s) are shown as a function of increasing embedding dimension m. D and K were estimated by averaging over embedding dimensions 14 to 18 (AF) and 18 to 22 (sinus rhythm).

of sinus rhythm such oscillations were not found. This is probably due to the fact that during AF the embedding window $T=(m-1)l\Delta t$ contains 4 to 8 AF intervals while there are only 1 to 2 in the case of sinus rhythm.

In tables II and III the correlation dimensions and correlation entropies are given as derived from the electrograms of the left and right atrium in five goats. No scaling regions were found in the correlation integrals during sustained AF (with exception of one RA electrogram in goat no. 4). After infusion of cibenzoline scaling regions were observed at relatively large distances of about [0.15;0.40] in phase space. Correlation dimension D estimated from right atrial electrograms ranged from 2.8 ± 0.2 to 4.1 ± 0.2. In the left atrium D ranged from 3.0 ± 0.2 to 4.4 ± 0.3. Correlation entropy ranged from 1.6 ± 0.2 to 6.2 ± 0.3 nats/s (left atrium), and from 2.6 ± 0.1 to 5.7 ± 0.3 nats/s (right atrium). Sinus rhythm was characterized by a correlation dimension D between 1.0 ± 0.1 and 1.9 ± 0.1, and a correlation entropy K

TABLE II. Effects of cibenzoline on correlation dimension. SAF indicates sustained atrial fibrillation; CIB25, CIB50, CIB85, atrial fibrillation during infusion of cibenzoline (see table I); LA, left atrium; RA, right atrium. Results are shown for atrial unipolar electrograms in which a scaling region was identified. Scaling regions were found at normalized distances of about [0.15;0.40] (AF) and [0.10;0.20] (sinus rhythm). Estimated values were averaged over embedding dimensions 14 to 18 (AF) and 18 to 22 (sinus rhythm), and are presented as mean (SD). Coherent averaging of far-field ventricular potentials was applied in episodes of AF.

Goat no.	Atrial fibrillation								Sinus rhythm
	SAF		CIB25		CIB50		CIB85		
	LA	RA	LA	RA	LA	RA	LA	RA	RA
1	–	–	–	–	4.1 (0.3)	–	–	–	1.21 (0.03)
	–	–	–	–	–	–	–	–	1.17 (0.03)
	–	–	–	–	–	–	–	–	1.06 (0.01)
	–	–	–	–	–	–	–	–	1.18 (0.03)
	–	–	–	–	–	–	–	–	1.15 (0.06)
2	–	–	–	3.4 (0.2)	4.2 (0.2)	3.8 (0.3)	–	4.0 (0.3)	–
	–	–	–	3.8 (0.2)	3.0 (0.2)	4.1 (0.3)	–	4.0 (0.3)	–
	–	–	–	3.1 (0.2)	–	–	–	–	–
	–	–	–	3.1 (0.2)	–	–	–	–	–
	–	–	–	–	–	–	–	–	–
3	–	–	3.6 (0.2)	3.3 (0.2)	4.4 (0.3)	3.7 (0.2)	4.2 (0.3)	4.1 (0.2)	1.4 (0.1)
	–	–	3.5 (0.2)	3.1 (0.2)	4.3 (0.3)	2.9 (0.2)	–	3.8 (0.2)	1.3 (0.1)
	–	–	–	3.6 (0.3)	–	3.3 (0.2)	–	3.5 (0.2)	1.5 (0.1)
	–	–	–	3.3 (0.2)	–	3.2 (0.2)	–	3.8 (0.2)	1.3 (0.1)
	–	–	–	3.6 (0.3)	–	2.8 (0.2)	–	3.6 (0.2)	1.5 (0.1)
4	–	3.0 (0.2)	3.9 (0.3)	3.4 (0.3)	4.1 (0.3)	4.1 (0.4)	4.3 (0.2)	4.0 (0.3)	–
	–	–	–	3.5 (0.3)	–	3.9 (0.3)	4.0 (0.2)	–	–
	–	–	–	–	–	3.8 (0.3)	3.6 (0.2)	–	–
	–	–	–	–	–	–	4.4 (0.3)	–	–
	–	–	–	–	–	–	–	–	–
5	–	–	–	–	–	–	–	–	1.9 (0.1)
	–	–	–	–	–	–	–	–	1.5 (0.1)
	–	–	–	–	–	–	–	–	1.4 (0.1)
	–	–	–	–	–	–	–	–	1.9 (0.1)
	–	–	–	–	–	–	–	–	1.6 (0.1)

between 0.48 ± 0.02 and 2.8 ± 0.3 nats/s. The two-dimensional phase plot of sinus rhythm shortly after cardioversion resembled noisy limit cycle behavior. However, low-dimensional chaotic dynamics can not be ruled out at present.

C. Coarse-grained analysis

Apart from the presence of low-dimensional features in the dynamics revealed by scaling regions, different ''types'' of dynamics may be identified by characterizing the correlation integral at a single distance r in phase space of embedding dimension m. This leads to coarse-grained estimates of the correlation dimension and entropy, which are indicators of the complexity of the dynamics. In figure 5, correlation integrals of AF were characterized at a distance r_{cg} ranging from 0.14 to 0.19 in phase space and at embedding dimension 10 (marked by an asterisk). Coarse-grained dimension D_{cg} during sustained AF was 3.6. With increasing dosages of cibenzoline, D_{cg} first decreased to 2.6 (CIB25), and then increased again to 3.9 (CIB50) and 3.5 (CIB85). Coarse-grained correlation entropy K_{cg} during sustained AF was 8.9 nats/s and gradually decreased during infusion of cibenzoline to 5.9 nats/s (CIB85). Sinus rhythm was characterized by the coarse-grained correlation dimension and entropy at $r_{cg} = 0.15$ and embedding dimension 20. The estimated values were $D_{cg} = 1.4$ and $K_{cg} = 0.8$ nats/s (figure 5).

Table IV gives the results of the coarse-grained analysis averaged over five electrograms from the left and the right atrium in five goats, respectively. Also, the average values of the left and right atrial coarse-grained correlation dimension D_{cg} and entropy K_{cg} are given. In the right atrium D_{cg} decreased from 4.9 ± 0.9 during sustained AF to 3.8 ± 1.3 at CIB25 (−22%), to 4.1 ± 1.4 at CIB50 (−16%) and to 4.6 ± 1.4 at CIB85 (−6%). In the left atrium the coarse-grained correlation dimension showed a progressive decrease from 5.5 ± 1.0 (sustained AF) to 4.8 ± 1.0 at CIB85 (−13%).

The coarse-grained correlation entropy K_{cg} progressively decreased both in the right and left atrium during infusion of cibenzoline from 9.3 ± 2.8 nats/s during sustained AF to 6.6 ± 2.0 nats/s (−29%) and from 10.2 ± 1.7 (sustained AF) to 6.8 ± 1.2 nats/s (−33%), respectively. The decrease in K_{cg} indicates an increased regularity in the recorded electrograms, partly due to a decreasing frequency of local atrial activation induced by cibenzoline. To account for the slowing of the rate of AF during infusion of cibenzoline, we also estimated the coarse-grained correlation entropy by

TABLE III. Effects of cibenzoline on correlation entropy. See table II for an explanation. Correlation entropy is expressed in units of nats/s.

Goat no.	Atrial fibrillation								Sinus rhythm
	SAF		CIB25		CIB50		CIB85		
	LA	RA	LA	RA	LA	RA	LA	RA	RA
1	–	–	–	–	4.4 (0.2)	–	–	–	0.48 (0.02)
	–	–	–	–	–	–	–	–	0.55 (0.01)
	–	–	–	–	–	–	–	–	0.65 (0.07)
	–	–	–	–	–	–	–	–	0.55 (0.02)
	–	–	–	–	–	–	–	–	0.93 (0.16)
2	–	–	–	3.7 (0.1)	2.6 (0.2)	5.3 (0.2)	–	5.2 (0.2)	–
	–	–	–	5.4 (0.3)	1.6 (0.2)	5.6 (0.2)	–	4.2 (0.1)	–
	–	–	–	5.3 (0.2)	–	–	–	–	–
	–	–	–	5.7 (0.3)	–	–	–	–	–
	–	–	–	–	–	–	–	–	–
3	–	–	4.4 (0.3)	4.2 (0.1)	4.7 (0.2)	3.1 (0.1)	3.8 (0.2)	3.3 (0.1)	1.3 (0.1)
	–	–	3.3 (0.1)	4.2 (0.2)	3.6 (0.1)	3.4 (0.1)	–	3.4 (0.1)	1.3 (0.2)
	–	–	–	4.1 (0.1)	–	3.3 (0.1)	–	2.6 (0.1)	1.1 (0.2)
	–	–	–	5.0 (0.3)	–	4.3 (0.3)	–	3.8 (0.1)	1.0 (0.2)
	–	–	–	4.5 (0.1)	–	4.6 (0.3)	–	4.4 (0.2)	1.6 (0.1)
4	–	5.0 (0.1)	6.2 (0.3)	3.9 (0.1)	5.4 (0.2)	3.0 (0.1)	4.8 (0.4)	2.6 (0.1)	–
	–	–	–	5.0 (0.1)	–	4.4 (0.1)	3.7 (0.3)	–	–
	–	–	–	–	–	4.0 (0.1)	4.9 (0.3)	–	–
	–	–	–	–	–	–	4.1 (0.3)	–	–
	–	–	–	–	–	–	–	–	–
5	–	–	–	–	–	–	–	–	2.0 (0.1)
	–	–	–	–	–	–	–	–	2.8 (0.3)
	–	–	–	–	–	–	–	–	2.4 (0.2)
	–	–	–	–	–	–	–	–	2.4 (0.1)
	–	–	–	–	–	–	–	–	2.7 (0.2)

multiplying K_{cg} by the mean AF interval. This ''scaled'' entropy K_{cg}^{s} is expressed in units of nats/cycle. The scaled entropy K_{cg}^{s} at the right atrium was 0.90 ± 0.26 during sustained AF, 0.85 ± 0.28 at CIB25 (-6%), 0.98 ± 0.35 at CIB50 ($+9\%$) and 1.19 ± 0.38 at CIB85 ($+32\%$). In the left atrium average values of K_{cg}^{s} were, respectively, 1.03 ± 0.21 (sustained AF), 0.93 ± 0.17 (CIB25, -10%), 1.00 ± 0.05 (CIB50, $+3\%$) and 1.25 ± 0.19 (CIB85, $+21\%$).

Analysis of variance showed that the minimum in D_{cg} during CIB25 at the right atrium was significantly different with respect to control. Although in the left atrium D_{cg} decreased from sustained AF to CIB85, this was found not to be statistically significant. Only in the left atrium the entropy K_{cg} (nats/s) during infusion of cibenzoline was statistically different from control. However in both the left and right atria, no significant differences were found when the entropy was scaled to the mean interval (nats/cycle).

D. Time reversibility

Although the values found for the correlation dimension and entropy point to the presence of low-dimensional features in the dynamics of AF induced by cibenzoline and of sinus rhythm shortly after cardioversion, these characteristics may still correspond to (linear) stochastic dynamics which mimics a low-dimensional process. Therefore, the electrograms were tested for the property of reversibility. All AF electrograms both before and after infusion of cibenzoline as well as the electrograms recorded during sinus rhythm were found to be irreversible (test statistic $S>3$). Thus, the hypothesis that these electrograms were generated by a static transformation of a linear Gaussian random process was rejected.

The dose dependent changes in the degree of reversibility caused by cibenzoline were quantified by estimating the distance Q between the original and time reversed delay vector distributions of the electrograms. Figure 6 shows Q averaged over the 5 electrograms selected at both the left and right atrium in five goats. At the right atrium, Q increased after the start of infusion of cibenzoline, reached a maximum and then relaxed towards the control value. In 4 out of 5 goats the maximum was reached soon after cibenzoline infusion had started (CIB25). Increased irreversibility by cibenzoline also occurred in the left atrium, although this effect was smaller than at the right atrium. Like in the right atrium, at higher levels of cibenzoline the dynamics of AF became more reversible again. Statistical analysis revealed no significant differences with respect to control. Q values during CIB25 and CIB85 were found to be significantly different in both the left and right atrium. Estimated Q values during sinus rhythm recorded shortly after conversion were 23.9 ± 2.8, 14.1 ± 1.1 and 7.7 ± 2.2 (mean $\pm$ standard error of mean, in units 10^{-3}) in goat nos. 1, 3 and 5, respectively.

TABLE IV. Effects of cibenzoline on coarse-grained correlation dimension and entropy. SAF indicates sustained atrial fibrillation; CIB25, CIB50, CIB85, atrial fibrillation during infusion of cibenzoline (see table I); LA, left atrium; RA, right atrium; D_{cg}, coarse-grained correlation dimension; K_{cg}, coarse-grained correlation entropy (nats/s). K^{s}_{cg}, coarse-grained correlation entropy scaled to the mean AF interval (nats/cycle). Results are presented as mean (SD), averaged over five atrial unipolar electrograms. Coherent averaging of far-field ventricular potentials was applied in episodes of AF. Coarse-grained quantities were estimated at a distance in phase space equal to the standard deviation of the electrogram divided by its peak-to-peak range and at embedding dimension 10 (AF) and 20 (sinus rhythm).

		Atrial fibrillation									
		SAF		CIB25		CIB50		CIB85		Sinus rhythm	
	Goat no.	LA	RA	LA	RA	LA	RA	LA	RA	LA	RA
D_{cg}	1	5.8 (0.6)	5.9 (0.8)	5.6 (0.8)	4.9 (0.5)	5.3 (1.4)	5.3 (0.7)	5.9 (0.8)	6.4 (0.4)	1.2 (0.2)	1.1 (0.2)
	2	6.4 (2.1)	4.9 (0.4)	5.5 (2.5)	2.9 (0.3)	6.2 (2.1)	3.5 (0.4)	5.7 (2.2)	4.1 (0.7)	–	–
	3	4.6 (2.3)	4.3 (0.6)	3.9 (0.6)	2.5 (0.2)	4.2 (1.2)	2.7 (0.7)	3.9 (0.9)	3.0 (0.7)	1.2 (0.3)	1.2 (0.1)
	4	4.3 (0.6)	3.8 (0.9)	3.4 (0.8)	3.3 (0.6)	3.9 (1.3)	3.0 (0.4)	3.6 (0.6)	4.1 (0.9)	–	–
	5	6.3 (1.6)	5.7 (0.7)	7.0 (0.4)	5.6 (0.8)	5.5 (0.8)	10.6 (2.1)	5.8 (0.8)	9.3 (1.7)	1.8 (0.6)	2.3 (0.3)
	Mean (SD)	5.5 (1.0)	4.9 (0.9)	5.1 (1.4)	3.8 (1.3) [a]	5.0 (1.0)	4.1 (1.4)	4.8 (1.0)	4.6 (1.4)	1.4 (0.4)	1.2 (0.2)
K_{cg}	1	10.6(3.9)	7.2(1.5)	6.3 (2.1)	6.1 (1.6)	7.5 (2.4)	6.0 (1.3)	6.0 (1.5)	7.4 (0.8)	0.8 (0.2)	0.5 (0.1)
	2	10.1(3.9)	13.7(2.6)	9.3 (1.3)	5.9 (1.7)	7.8 (3.4)	6.8 (2.3)	8.7 (1.2)	6.6 (1.0)	–	–
	3	8.6(3.9)	7.0(1.7)	6.6 (1.5)	5.9 (1.3)	6.3 (1.6)	5.0 (1.2)	6.8 (0.9)	5.4 (1.0)	0.9 (0.2)	1.1 (0.2)
	4	8.8(2.4)	8.0(2.9)	7.1 (2.0)	5.4 (1.1)	7.0 (1.5)	4.4 (1.0)	6.8 (1.0)	4.1 (1.0)	–	–
	5	12.8(1.8)	10.5(4.4)	9.0 (1.0)	12.1 (2.1)	6.5 (0.6)	10.6 (2.1) 5.8 (0.8)	9.3 (1.7)	1.8 (0.6)	2.3 (0.3)	
	Mean (SD)	10.2(1.7)	9.3(2.8)	7.7 (1.4) [a]	7.1 (2.8)	7.0 (0.6) [a]	6.6 (2.4)	6.8 (1.2) [a]	6.6 (2.0)	1.2 (0.6)	1.3 (0.9)
K^{s}_{cg}	1	1.03(0.38)	0.75(0.15)	0.69 (0.23)	0.77 (0.20)	1.03 (0.33)	0.97 (0.20)	1.11 (0.27)	1.44 (0.15)	0.49 (0.14)	0.31 (0.09)
	2	0.97(0.37)	1.31(0.25)	1.06 (0.15)	0.69 (0.20)	1.11 (0.49)	0.98 (0.33)	1.59 (0.22)	1.18 (0.19)	–	–
	3	0.92(0.42)	0.71(0.17)	0.92 (0.21)	0.80 (0.17)	0.99 (0.24)	0.77 (0.19)	1.22 (0.16)	0.95 (0.17)	0.45 (0.10)	0.57 (0.12)
	4	0.85(0.23)	0.74(0.27)	0.86 (0.24)	0.66 (0.14)	1.01 (0.22)	0.63 (0.14)	1.18 (0.17)	0.70 (0.17)	–	–
	5	1.39(0.19)	1.00(0.43)	1.11 (0.12)	1.35 (0.24)	1.05 (0.10)	1.54 (0.30)	1.15 (0.15)	1.66 (0.30)	0.80 (0.29)	1.04 (0.20)
	Mean (SD)	1.03(0.21)	0.90(0.26)	0.93 (0.17)	0.85 (0.28)	1.00 (0.05)	0.98 (0.35)	1.25 (0.19)	1.19 (0.38)	0.58 (0.19)	0.64 (0.37)

[a] $p < 0.05$ with respect to control.

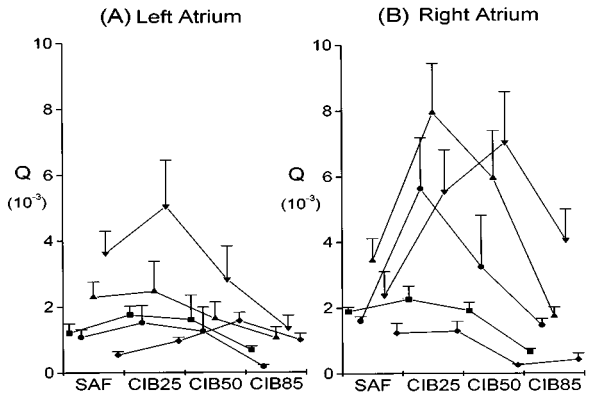

FIG. 6. The distance Q between the delay vector distributions of the original and time reversed electrograms at the left (a) and right atrium (b) during sustained atrial fibrillation (SAF) and during infusion of cibenzoline (CIB25, CIB50, CIB85). In the five goats Q reached a maximum at a relatively low dose of cibenzoline, and the degree of irreversibility of the dynamics was increased. At higher levels of cibenzoline the dynamics became more reversible again. The figure shows that time reversibility was more affected at the right atrium than at the left atrium. The results are averages over 5 electrograms and are presented as the mean $\pm$ standard error of the mean. Note that the curves of different goats are slightly shifted horizontally for the sake of a clear graphical presentation. Symbols ■,●,▲,▼,◆ correspond to the results of goat nos. 1 to 5, respectively.

IV. DISCUSSION

We start this discussion with a brief summary of characteristics of short-lasting, spontaneously terminating atrial fibrillation (paroxysmal AF) determined from a high-density mapping study in humans[36] and from a nonlinear analysis of AF electrograms in the same group of patients.[20] Some of the findings of these studies will be related to the results of the present study.

A. Characteristics of paroxysmal AF

A recent intra-operative high-density mapping study in WPW patients[36] showed that electrically induced, spontaneously terminating AF is a heterogeneous arrhythmia. Activation patterns were associated with a spectrum of spatio-temporal complexity, in which the number and size of intra-atrial reentry circuits varies considerably. Local activation ranged from relatively simple atrial activation patterns, in which the atrial myocardium acted passively, conducting wavelets arriving from active remote regions, to highly complex patterns during locally fully developed AF. A classification into at least three types (I, II, III) was proposed[36] based on the degree of complexity observed in high-density maps of AF. Type I was characterized by broad, uniformly propagating wavefronts activating the mapping electrode without a conduction delay. In type II one wave which was delayed considerably by an area of conduction block and/or a region of slow conduction, or two wavelets were observed. Type III of AF was characterized by a highly complex activation pattern, in which the mapped area was activated by three or more wavelets in the presence of multiple lines of conduction block.

In a separate study, nonlinear analysis was performed on single AF electrograms selected from this group of patients.[20] A scaling region in the correlation integral was only observed in type I of AF. The mapping area is then activated by broad depolarization waves which continuously change their main course of direction. It is therefore likely that scaling regions are a manifestation of discrete activation complexes in electrograms associated with single, uniformly conducting wavefronts passing the electrode without conduction delay.

To compare the dynamics associated with types I–III of AF, the coarse-grained correlation dimension D_{cg} and entropy K_{cg} were estimated. It was found that both D_{cg} and K_{cg} gradually increased from type I to type III of AF. The characterization based on the coarse-grained nonlinear complexity measures correlated well with the classification based on the degree of complexity visualized from high-density mapping.

B. Characteristics of sustained AF

In the present study no scaling regions were observed during sustained AF, so that the plaque electrodes probably were seldom activated by uniformly propagating waves (type I) during the process of self-sustained, ongoing AF. Also, coarse-grained correlation dimension and entropy were smaller than estimated from electrograms of type III AF in patients, for which $D_{cg}>6$ and $K_{cg}>14$ nats/s.[20] This suggests that sustained AF may be characterized as type II fibrillation. Thus sustained AF in electrically remodeled normal atria seems of an intermediate level of complexity, in which during most of the time a single wave associated with a considerable amount of conduction block and/or a region of slow conduction, or two wavelets are present in the mapped area.

C. Effects of cibenzoline on the dynamics of sustained AF

One of the features that distinguished AF during administration of cibenzoline from sustained AF was the presence of scaling regions in the correlation integrals during infusion of the drug. In three goats, scaling was observed in one or more electrograms during administration of cibenzoline, indicating that features of low-dimensional dynamics were present throughout the experiment. The correlation dimension D and correlation entropy K were similar to those estimated during type I of AF in humans.[20]

Coarse-grained analysis also showed that cibenzoline already had effect on the complexity of AF on the time scale of the shortest AF intervals. Notably, at the right atrium D_{cg} went through a minimum shortly after start of infusion (-22% at CIB25), followed by a slight relaxation (-13% at CIB85). At the left atrium, D_{cg} remained close to the control value (-6% at CIB85).

The coarse-grained correlation entropy was calculated in two different ways. The coarse-grained entropy K_{cg} (nats/s) is sensitive to the beat-to-beat changes in the rate of AF. The decrease of K_{cg} throughout the transition at least partly characterizes the lengthening of the fibrillation interval and the

decrease of the conduction velocity induced by cibenzoline. To account for the changing rate of AF, coarse-grained correlation entropy was scaled to the mean AF cycle length. The scaled entropy K_{cg}^{s} (nats/cycle) may be used as a measure of the interbeat morphological regularity of the electrogram configuration. It was shown that at both the left and right atrium a minimum in the scaled entropy occurred at CIB25 (-5% to -10%) followed by a steady increase ($+21\%$ to $+32\%$ at CIB85). This indicates that the morphology of AF electrograms became more uniform shortly after the start of infusion of cibenzoline. The reversibility test indicated that this was accompanied by an increased degree of irreversibility in the dynamics of AF. During the remainder of the experiment, the degree of irregularity in the waveform of AF electrograms increased again. This is in agreement with the observed increase of reversibility in the AF dynamics at higher levels of cibenzoline.

The nonlinear analysis suggested that cibenzoline did not drastically change the topology of the reconstructed dynamics: the structure of the phase plots (figure 5) was not substantially altered during the experiment and the dimensional complexity, characterized by D_{cg}, remained close to control. However, cibenzoline doubled the mean fibrillation interval with respect to control (table I). This affected the flow of the dynamics during AF: the velocity of points along the trajectory in phase space was progressively decreasing with an increasing dose of cibenzoline. As a result, the coarse-grained correlation entropy K_{cg} (nats/s) decreased with about 30% (CIB85) in both the left and right atrium.

The minimum in the coarse-grained parameters D_{cg} and K_{cg}^{s} (adjusted for the changing rate of AF) observed at CIB25 shows that cibenzoline made the dynamics of sustained AF less complex, followed by a relaxation towards the dynamical behavior during control. Also, scaling regions appeared in the correlation integrals of one or more electrograms (3 out of 5 goats) shortly after the start of infusion (CIB25). These low-dimensional features in the dynamics persisted during the remainder of the experiments, corresponding to an increased global organization in atrial activation during sustained AF. Furthermore, the reversibility measure Q indicated that the dynamics was more irreversible shortly after the infusion of cibenzoline (CIB25), followed by a relaxation towards the control dynamics. These effects seemed to be more pronounced at the right atrium than at the left atrium. However, analysis of variance revealed that of the changes in the coarse-grained parameters D_{cg}, K_{cg}^{s} and the reversibility measure Q, only D_{cg} at CIB25 was significantly different from control (sustained AF) at the 0.05 level.

We conclude from the nonlinear analysis that cibenzoline did not induce appreciable alterations in the dynamics of sustained AF, other than a slowing down of the process of electrical atrial activation. A minor effect was the occurrence of increased global organization of AF induced shortly after the start of drug administration. The above findings suggest the idea that to a first approximation the dynamics of sustained atrial fibrillation and the dynamics up to CIB85 can be considered ''orbitally equivalent'' (cf. Ref. 37).

The population of five goats as used in this study was rather inhomogeneous with respect to the duration of sustained AF. The effects of cibenzoline on the AF dynamics seemed to be more pronounced when the episode of sustained fibrillation had lasted longer. Considering for example the effects in the right atrium, scaling regions were present during infusion of cibenzoline in all electrograms of goat no. 3 (sustained AF duration 115 days), while no scaling was identified in electrograms of goat 1 and 5 (sustained AF duration 4 and 8 days). Similarly, time reversibility was affected more clearly in the right atrium of goat no. 3 than in goat nos. 1 and 5, despite the fact that the total dose of cibenzoline in these goats was about the same (table I).

D. Relation to the mechanism of AF

According to the multiple wavelet hypothesis,[38] the mechanism of self-sustained AF is based on the presence of a number of short-lived wavelets which travel randomly through the atrial myocardium. This has been verified experimentally by mapping studies,[39,40] in which it was shown that wavefronts continuously reenter and excite areas that were previously excited either by themselves or by other wandering wavelets, thus confirming that random reentry[41] is the basic mechanism for AF.

It was shown that sustained AF in a goat model of pacing induced fibrillation is not consistent with a state of fully developed AF (type III), but rather seems to be of a level of moderate complexity (type II) where the mapped area is continuously invaded by a single, nonuniformly conducting wavefront or two wavelets. Shortly after the start of infusion, in 3 out of 5 goats scaling regions were present in the correlation integrals of one or more electrograms, probably resulting from single broad activation waves sweeping across the mapped area. These type I characteristics point to an increased global organization of AF. This effect persisted during the remainder of the experiment which may indicate a decrease in the number and an increase in the size of intra-atrial circuits. It is therefore likely that perpetuation of AF in these goats was maintained by a few macro-reentrant circuits. However, in 2 out of 5 goats scaling regions were not observed, so that in these goats the mapping area probably was still invaded by one wavefront associated with a conduction block and/or a region of slow conduction, or two wavelets (AF type II) most of the time.

The results of the temporal nonlinear analysis of single local electrograms of sustained AF in goats have been linked to a scale of spatial organization (types I–III) deduced from high-density mapping of atrial activation patterns during paroxysmal AF in humans.[36] Thus aspects of temporal organization are directly linked to spatial organization. This is a reasonable assumption, since we have shown in a previous study[20] that a characterization of electrograms by nonlinear time series analysis is consistent with the classification of AF into three types (I–III) based on the degree of spatiotemporal complexity of atrial activation patterns. However, it is uncertain to what extent the time series analysis of sustained AF in goats may be compared to spatial analysis of paroxysmal AF in humans. To this end, the results of the nonlinear analysis

have to be supplemented with atrial activation maps in the goat model of sustained AF.

The effects of class Ic drugs on activation patterns during vagally induced, acute atrial fibrillation in anesthetized open-chest dogs were studied by Nattel and coworkers,[42,43] who showed that shortly after the start of drug infusion atrial activation was more homogeneous. In their experiments the anti-arrhythmic agents always regularized AF by increasing the size and reducing the number of simultaneous reentry circuits, until one or two large macro-reentrant circuits remained. Brugada *et al.*[21] performed intra-operative mapping in a patient with chronic atrial fibrillation during administration of cibenzoline. It was shown that a single broad wavefront was circulating around the caval veins in the right atrium shortly after infusion had ended. The left atrium acted as a passive bystander, and was activated by the right atrial macro-circuit from different directions. Also, Kirchhof *et al.*[44] reported that the class Ic drug ORG 7797 prolonged the minimal path length that is covered by wavelets during very high pacing rates in instrumented conscious dogs, resulting in an increase in size and decrease of the number of reentrant circuits.

These electrophysiological studies point out that class Ic drugs seem to enhance the organization of atrial activation during AF, which occurs on the scale of the shortest AF intervals. The nonlinear analysis of electrograms in a goat model of chronic AF supports these observations: increased global ordering during AF was indicated early in the experiments (CIB25) by scaling regions in correlation integrals and a minimum in the coarse-grained correlation dimension and scaled coarse-grained correlation entropy.

In the present study we have shown that no major changes in the dynamics of sustained AF were detected after drug loading, apart from a deceleration of the atrial activation process and a certain degree of global ordering of AF induced at a relatively low dose of cibenzoline. From these observations it is not clear which factor triggers the conversion to sinus rhythm. We speculate that, via the depressed excitability of atrial tissue, the lowering of the safety factor for conduction[45] induced by the administration of cibenzoline results in a diminution of the curvature of circulating wavefronts. Consequently, wavelets are gradually forced to travel along wider arcs through the myocardium. When a critical value of curvature[46] is reached, the ends of wavefronts cannot curl anymore and wavefronts will effectively run like planar waves until the borders of the atria are reached and get extinguished. When the number of wavelets gets smaller than necessary to support the perpetuation of random reentry, AF terminates and sinus rhythm is restored. These critical events would occur in a short period of time, just before conversion to sinus rhythm takes place. This mechanism of the transition is reminiscent of a bifurcation induced by cibenzoline. The hallmark of a bifurcation is a sudden qualitative change in the dynamical behavior as a control parameter goes through a critical value. As suggested by the theory of excitable media,[46–48] the control parameter might be $\epsilon = \tau_u / \tau_v$, which is the product of measures of excitability (governed by the time constant τ_u of the fast activation process) and refractoriness (governed by the time constant τ_v of the recovery process) of atrial tissue. The parameter ϵ appears in the equations of reaction-diffusion models of excitable media which are extensively used in the study of cardiac excitation (see Gray and Jalife[49] for a review). Although the relation of model parameters to observable electrophysiological quantities is by no means trivial,[50] information about the control parameter might be contained in experimental parameters like for instance the rate of the rise of the upstroke of the extracellular action potential (measure of the fast activation variable) and the effective refractory period (measure of the slow inhibitor variable in reaction-diffusion models).

E. Concluding remarks

Since the early eighties the analysis of time series has received a great impetus from the developments in the theory of nonlinear dynamical systems and a wealth of methods has been described to characterize the time series generated by known low-dimensional chaotic systems. However, time series from the natural world are always a mixture of deterministic and random features, and the main challenge of nonlinear time series analysis is the disentangling of these features. In this respect the limitations of the current methods based on ''chaos theory'' for the analysis of experimental data are by now well recognized and are mainly due to a lack of statistical foundation of estimation and inference methods.

Recently, statisticians have become interested in the analysis of time series using concepts from nonlinear dynamical systems theory and a statistical nonlinear time series analysis is currently being developed.[51] In its present form the nonlinear methods are nevertheless useful since the results are directly related to properties of the dynamics generating the observed time series. In particular, it might be rewarding to explore the connection of nonlinear measures in reconstructed phase space with characteristics of the process taking place in physical space.[52]

It is often remarked that most if not all results from the nonlinear time series analysis can be surmised from a graph of the experimental data. However, the aim of any time series analysis is to provide *quantitative* measures characterizing the observed time series, and this cannot be achieved with the naked eye. In this respect, nonlinear time series analysis can already make a meaningful contribution especially in discriminating between time series, although a thorough exploration and critical evaluation of the methods at hand are still needed.[53]

In this paper the application of nonlinear analysis to scalar epicardial atrial electrograms has suggested that the dynamics during sustained AF and after modification by cibenzoline up to CIB85 can be regarded as orbitally equivalent to a first approximation. It is therefore expected that the spatiotemporal complexity of atrial activation patterns as visualized from epicardial mapping would roughly remain the same, apart from a decreasing velocity of propagating activation fronts. Our findings suggest that it would be extremely interesting to study drugs which do not leave the

dynamics orbitally equivalent. Possible candidates are drugs with electrophysiological properties different from class I drugs, like for example the class III agent sotalol.

The insights gained from nonlinear time series analysis and electrophysiological measurements by themselves are not sufficient to explain the anti-arrhythmic effects of drugs in all detail. However, the concerted results from both electrophysiological measurements and time series analysis together with mathematical modelling of the pharmacological conversion of AF may lead to a better understanding of the dynamics of anti-fibrillatory drug action and the mechanisms leading to the termination of atrial fibrillation.

ACKNOWLEDGMENTS

We would like to thank Rik Dorland and Maurits Wijffels for their help with the data selection. We wish to thank Dr. N. Kormoss from Continental Pharma/Searle (Belgium) for supplying cibenzoline and Jan van Hartevelt, Jan Hollen and Frits Schmitz for their assistance with the extension of the data acquisition system. This study was supported by Grant No. 805-06-181 from the Life Sciences Foundation (SLW), which is subsidized by the Netherlands Organization for Scientific Research (NWO).

APPENDIX: IMPLEMENTATION OF THE NUMERICAL PROCEDURES

In this section we give a detailed description of the procedure to calculate the atrial template containing the far-field ventricular potential. Furthermore, the Grassberger-Procaccia (GP) method is elucidated which is used to estimate the correlation integral, the correlation dimension and correlation entropy from the recorded electrograms. Also, the test for reversibility is described here.

1. Coherent averaging of the ventricular response

The R-wave was detected in a left ventricular electrogram (LV). To this end the LV electrogram was first smoothed using a moving average filter, viz.

$$y(t_i)=\frac{1}{2M+1}\sum_{k=-M}^{M} v(t_{i+k}), \tag{A1}$$

where $v(t_i)$ is taken from the LV electrogram, and $y(t_i)$ is the filter output at a sample time $t_i=i\Delta t$, where Δt is the sample interval. The width of the smoothing window M was set equal to 10. The time derivative of the filtered signal was calculated as $y'(t_i)=y(t_i)-y(t_{i-1})$. The value t_i corresponding to the largest negative value of $y'(t_i)$ was taken to represent the moment of occurrence of the R-wave.

In the smoothed LV electrogram, the signal was averaged in all time windows around the detected R-waves. We visually selected a time segment from this averaged signal and the template of the far-field ventricular potential was obtained by averaging the deflections in the corresponding time segments in the atrial electrogram.

This template was smoothed using a moving averaging filter [equation (A1), $M = 5$]. The filtered template was multiplied by a taper function to force the edges of the template to the baseline. The taper function is given by

$$h(t_i)=\begin{cases} 0.5-0.5\cos\left(\dfrac{10\pi t_i}{T}\right), \\ \qquad \text{if } 0\leqslant t_i\leqslant 0.1T \text{ or } 0.9T\leqslant t_i\leqslant T, \\ 1, \quad \text{if } 0.1T<t_i<0.9T, \end{cases} \tag{A2}$$

where T is the length of the template segment. Finally, the template was subtracted from the atrial electrogram in time windows of length T centered at the detected R-waves to remove the far-field ventricular potentials.

2. Estimating the correlation integral

It has been shown that the correlation integral of a (chaotic) deterministic system is given by[54]

$$C_m(r)=Ar^D e^{-mlK\Delta t}, \tag{A3}$$

where A is a constant, D the correlation dimension, K the correlation entropy, m the embedding dimension, l the embedding delay and Δt the sample interval. Equation (A3) is valid for sufficiently small distance r in phase space and sufficiently large embedding dimension m.

The correlation integral is estimated as

$$C_m(N,r)=\frac{1}{N_{\text{dis}}}\sum_{i\in\{i_{\text{ref}}\}}\sum_{|j-i|\geqslant W}\Theta(r-\|\vec{x}(i)-\vec{x}(j)\|), \tag{A4}$$

where $N=L-(m-1)l$ is the number of delay vectors [equation (1)] resulting from a time series of length L in reconstructed phase space of embedding dimension m. The Heaviside function Θ is 1 for positive arguments and 0 otherwise. The norm $\|\cdot\|$ denotes the distance between two delay vectors. The supremum norm,

$$\|\vec{x}(i)-\vec{x}(j)\|=\max_{0\leqslant k<m}|x(i+k)-x(j+k)|, \tag{A5}$$

was used to calculate the distance between delay vectors.

The inner sum in equation (A4) counts the number of delay vectors within a distance r from a reference vector. The outer sum adds the results over a set $\{i_{\text{ref}}\}$ of reference vectors and the normalization factor N_{dis} is the total number of distances involved in the summations. We used 10000 randomly chosen reference vectors, which is equal to one third of the number of samples in the time series (sampled down to 30000 samples) as suggested by Theiler.[55] An optimized algorithm was used to search for neighboring vectors in reconstructed phase space.[28] Before calculating the correlation integral, the time series was rescaled such that the difference between the minimal and maximal value of the time series becomes one. The distances calculated were discretized at a resolution of 16 divisions per binade.

A parameter $W\geqslant 1$ (the Theiler correction) was included in equation (A4) to prevent false contributions to the correlation integral resulting from the linear correlation between successive delay vectors in reconstructed phase space.[27] In the calculation of correlation integrals, distances from vector

pairs $(\vec{x}(i),\vec{x}(j))$ were excluded when $|i-j|<W$. The parameter W was set equal to twice the lag corresponding to the first minimum of the mutual information function.

3. Estimating correlation dimension and entropy

The correlation integral is plotted on a double logarithmic scale (base 10) as a function of distance r. In such a plot, one then looks for a linear part, the so-called ''scaling region,'' at a given embedding dimension m. The correlation dimension D_m was estimated as the slope in the scaling region using linear regression through points $(\ln r, \ln C_m(r))$.

The correlation entropy K_m was calculated fitting the GP model [equation (A3)]. A nonlinear Levenberg-Marquardt fit procedure was applied, estimating K_m simultaneously from $C_m(r)$ within the scaling region at two consecutive values of m. Assuming that the calculated distances are independent, the correlation integral was fitted with a weighting factor $\sqrt{C_m(r)\cdot(1-C_m(r))}$ following Theiler.[55]

Correlation dimension and entropy were averaged over five values in the range of convergence. In electrograms of AF, D_m and K_m were averaged over embedding dimensions 14 to 18. During sinus rhythm the results were averaged over embedding dimensions 18 to 22.

A drawback of the nonlinear analysis is that in general at present the time series algorithms are data ''hungry'' and computationally demanding. In this study, one minute recordings sampled at 1 kHz were sampled down to $L=30000$ to somewhat reduce the computational effort to estimate the correlation dimension and entropy. According to a criterium proposed by Eckmann and Ruelle[56] values of the correlation dimension up to $(-2\log N)/\log r$ at a resolution r in reconstructed phase space are still reliable using the Grassberger-Procaccia algorithm. This yields an upper limit for the correlation dimension of 9 for distances of about 0.1. The dimensional values reported here were significantly smaller, which suggests that the number of samples used was sufficient.

The coarse-grained correlation dimension is defined by

$$D_m(r)=\frac{d\ln C_m(r)}{d\ln(r)}, \tag{A6}$$

which is estimated by linear regression through three consecutive points $(\ln(r), \ln C_m(r))$.

The coarse-grained correlation entropy is defined by the logarithm of the quotient of two correlation integrals at embedding dimensions m and $m+n$, viz.,

$$K_m(r)=\frac{1}{n\not{\ell}\Delta t}\ln\left(\frac{C_m(r)}{C_{m+n}(r)}\right), \tag{A7}$$

where n is a fixed integer, l the embedding delay and Δt the sample interval. To reduce statistical fluctuations, we set $n=2$ in equation (A7).

The coarse-grained correlation dimension and entropy were evaluated at a distance r_{cg} in phase space, which was equal to the standard deviation of the electrogram divided by the largest absolute difference of its amplitude. The embedding dimension m was chosen 10 for electrograms of AF and 20 for electrograms of sinus rhythm. The coarse-grained correlation dimension and entropy for these values of m and r_{cg} are denoted by D_{cg} and K_{cg}, respectively.

4. Test for time reversibility

Consider delay vectors $\vec{x}(i)$ [equation (1)] constructed from a stationary time series $\{v(i)\}_{i=1}^{L}$ of length L. The time series is reversible if the probability distribution $\rho(\vec{x})$ of the delay vectors is invariant under time reversal for all m and l, i.e.

$$\rho(P\vec{x})=\rho(\vec{x}), \tag{A8}$$

where P denotes the time reversal operator defined as

$$P:(v_i,v_{i+l},\ldots,v_{i+(m-1)l})\mapsto(v_{i+(m-1)l},\ldots,v_{i+l},v_i). \tag{A9}$$

The square Q of a distance measure between the time forward and time reversed distributions is defined, viz.

$$Q=\frac{1}{2}(d\sqrt{\pi})^m\int d\vec{x}[\rho'(\vec{x})-\rho'(P\vec{x})]^2, \tag{A10}$$

where d denotes the bandwidth and $\rho'(\vec{x})$ is

$$\rho'(\vec{x})=\left(\frac{2}{\pi d^2}\right)^{m/2}\int d\vec{r}\ \rho(\vec{x})\ \exp\left(\frac{-2|\vec{x}-\vec{r}|^2}{d^2}\right). \tag{A11}$$

In the calculations an unbiased estimator $\widehat{Q}$ of Q was used, given by

$$\widehat{Q}=\frac{2}{N(N-1)}\sum_{i<j}w_{ij}, \tag{A12}$$

where

$$w_{ij}=\exp(-|\vec{x}_i-\vec{x}_j|^2/d^2)-\exp(-|\vec{x}_i-P\vec{x}_j|^2/d^2), \tag{A13}$$

and $N=L-(m-1)l$. Under the null hypothesis (H_0) of reversibility the expected value of $\widehat{Q}$ is equal to 0 with a standard deviation given by

$$\sigma=\frac{2}{N(N-1)}\left(\sum_{j<i}w_{ij}^2\right)^{1/2}. \tag{A14}$$

The test statistic S is defined as

$$S=\frac{\widehat{Q}}{\sigma}. \tag{A15}$$

Under the H_0, S has expected value 0 and unit standard deviation. In the derivation of these results, it was assumed that samples from the delay vector distributions are independent. In order to reduce the effect of dependences, we excluded all pairs (i,j) from the calculation of S which are closer in time than some lag W (cf. the calculation of correlation integrals). Furthermore, higher order dependences between delay vectors were suppressed by comparing nonoverlapping segments consisting of $\not{\ell}$ consecutive delay vectors,

instead of single pairs of delay vectors.[57] Consequently, in the calculation of $\widehat{Q}$ the terms w_{ij} are replaced by

$$w'_{i',j'} = \frac{1}{\ell^2} \sum_{p=1}^{\ell} \sum_{q=1}^{\ell} w_{i'\ell+p,j'\ell+q}. \tag{A16}$$

The test parameters for electrograms of AF were chosen as follows. The embedding delay l was set equal to the lag corresponding to the first minimum of the mutual information function. Embedding dimension was $m = 5$, Theiler correction $W = 4l$, segment length $\ell = 8l$ and bandwidth $d = 0.5\sigma$, where σ is the standard deviation of the time series. This setting was also used for the analysis of electrograms during sinus rhythm, however the embedding delay was set to 5 times the lag corresponding to the first minimum of the mutual information. With these parameter settings, the Theiler correction W and segment length ℓ covered about 1 to 3 and 2 to 6 times the length of the mean interval, respectively. Prior to the calculations, electrograms were sampled down to $L = 10000$ points.

[1] S. H. Hohnloser and Y.-G. Li, ''Drug treatment of atrial fibrillation: What have we learned?'' Current Opinion Cardiol. **12**, 24–32 (1997).

[2] A. E. Epstein, A. P. Hallstrom, W. J. Rogers, P. R. Liebson, A. A. Seals, J. L. Anderson, J. D. Cohen, R. J. Capone, and D. G. Wyse for the Cardiac Arrhythmia Suppression Trial Investigators, ''Mortality following ventricular arrhythmia suppression by encainide, flecainide, and moricizine after myocardial infarction,'' J. Am. Med. Assoc. **270**, 2451–2455 (1993).

[3] T. R. Chay, ''Bifurcations in heart rhythms,'' Int. J. Bifurcation Chaos **5**, 1439–1486 (1995).

[4] C. F. Starmer, A. A. Lastra, V. V. Nesterenko, and A. O. Grant, ''Proarrhythmic response to sodium channel blockade. Theoretical model and numerical experiments,'' Circulation **84**, 1364–1377 (1991).

[5] C. F. Starmer, D. N. Romashko, R. S. Reddy, Y. I. Zilberter, J. Starobin, A. O. Grant, and V. I. Krinsky, ''Proarrhythmic response to potassium channel blockade. Numerical studies of polymorphic tachyarrhythmias,'' Circulation **92**, 595–605 (1995).

[6] M. O. Arnsdorf and G. J. Sawicki, ''Flecainide and the electrophysiologic matrix: The effects of flecainide acetate on the determinants of cardiac excitability in sheep purkinje fibers,'' J. Cardiovasc. Electrophysiol. **7**, 1172–1182 (1996).

[7] Y. Cha, A. Wales, P. Wolf, S. Shahrokni, N. Sawhney, and G. K. Feld, ''Electrophysiological effects of the new class III antiarrhythmic drug dofetilide compared to the class IA antiarrhythmic drug quinidine in experimental canine atrial flutter: Role of dispersion of refractoriness in antiarrhythmic efficacy,'' J. Cardiovasc. Electrophysiol. **7**, 809–827 (1996).

[8] E. M. Vaughan Williams, ''Classification of anti-arrhythmic drugs,'' in *Cardiac Arrhythmias*, edited by E. Sandoe, E. Flensted-Jense, and K. H. Olesen (Astra, Sodertalie Sweden, 1970), pp. 449–472.

[9] E. Ott, *Chaos in Dynamical Systems* (Cambridge University Press, Cambridge, 1993).

[10] E. Ott, T. Sauer, and J. A. Yorke, *Coping with Chaos; Analysis of Chaotic Data and the Exploitation of Chaotic Systems* (Wiley, New York, 1994).

[11] H. D. I. Abarbanel, R. Brown, J. L. Sidorowich, and L. Sh. Tsimring, ''The analysis of observed chaotic data in physical systems,'' Rev. Mod. Phys. **65**, 1331–1392 (1993).

[12] P. Grassberger, T. Schreiber, and C. Schaffrath, ''Nonlinear time sequence analysis,'' Int. J. Bifurcation Chaos **1**, 521–547 (1991).

[13] F. Ravelli and R. Antolini, ''Complex dynamics underlying the human electrocardiogram,'' Biol. Cybern. **67**, 57–65 (1992).

[14] D. T. Kaplan and R. J. Cohen, ''Is fibrillation chaos?,'' Circ. Res. **67**, 886–892 (1990).

[15] F. X. Witkowski, K. M. Kavanagh, P. A. Penkoske, R. Plonsey, M. L. Spano, W. L. Ditto, and D. T. Kaplan, ''Evidence for determinism in ventricular fibrillation,'' Phys. Rev. Lett. **75**, 1230–1233 (1995).

[16] P. van Leeuwen, H. Bettermann, U. an der Heiden, and H. C. Kümmell, ''Circadian aspects of apparent correlation dimension in human heart rate dynamics,'' Am. J. Physiol. **269**, H130–H134 (1995).

[17] P. I. Saparin, M. A. Zaks, J. Kurths, A. Voss, and V. S. Anishchenko, ''Reconstruction and structure of electrocardiogram phase portraits,'' Phys. Rev. E **54**, 737–742 (1996).

[18] T. Schreiber and D. T. Kaplan, ''Nonlinear noise reduction for electrocardiograms,'' Chaos **6**, 87 (1996).

[19] A. Casaleggio, A. Corana, R. Ranjan, and N. V. Thakor, ''Dimensional analysis of the electrical activity in fibrillating isolated hearts,'' Int. J. Bifurcation Chaos **6**, 1547–1561 (1996).

[20] B. P. T. Hoekstra, C. G. H. Diks, M. A. Allessie, and J. DeGoede, ''Nonlinear analysis of epicardial atrial electrograms of electrically induced atrial fibrillation in man,'' J. Cardiovasc. Electrophysiol. **6**, 419–440 (1995).

[21] J. Brugada, S. Gürsoy, P. Brugada, J. Atié, G. Guiraudon, and E. Andries, ''Cibenzoline transforms random re-entry into ordered re-entry in the atria,'' Eur. Heart. J. **14**, 267–272 (1993).

[22] M. C. E. F. Wijffels, C. J. H. J. Kirchhof, R. Dorland, and M. A. Allessie, ''Atrial fibrillation begets atrial fibrillation. A study in awake chronically instrumented goats,'' Circulation **92**, 1954–1968 (1995).

[23] F. Takens, ''Detecting strange attractors in turbulence,'' in *Dynamical Systems and Turbulence (Warwick 1980)*, Lecture Notes in Mathematics, edited by D. A. Rand and L.-S. Young (Springer, Berlin, 1981), vol. 898, pp. 366–381.

[24] A. M. Fraser and H. L. Swinney, ''Independent coordinates for strange attractors from mutual information,'' Phys. Rev. A **33**, 1134–1140 (1986).

[25] P. Grassberger and I. Procaccia, ''Measuring the strangeness of strange attractors,'' Physica D **9**, 189–208 (1983).

[26] F. Takens, ''Invariants related to dimensions and entropy,'' Atas do 13. Coloquio Brasileiro de Matematica, 1983, pp. 353–359.

[27] J. Theiler, ''Spurious dimensions from correlation algorithms applied to limited time-series data,'' Phys. Rev. A **34**, 2427–2432 (1986).

[28] P. Grassberger, ''An optimized box-assisted algorithm for fractal dimensions,'' Phys. Lett. A, **148**, 63–68 (1990).

[29] M. Ding, C. Grebogi, E. Ott, T. Sauer, and J. A. Yorke, ''Plateau onset of correlation dimension: When does it occur?,'' Phys. Rev. Lett. **70**, 3872–3875 (1993).

[30] J. G. Caputo and P. Atten, ''Metric entropy: an experimental means for characterizing and quantifying chaos,'' Phys. Rev. A **35**, 1311–1316 (1987).

[31] S. Pincus, ''Approximate entropy (ApEn) as a complexity measure,'' Chaos **5**, 110–117 (1995).

[32] D. T. Kaplan, M. I. Furman, S. M. Pincus, S. M. Ryan, and L. A. Lipsitz, ''Aging and the complexity of cardiovascular dynamics,'' Biophys. J. **59**, 945–949 (1991).

[33] P. Gaspard and X.-J. Wang, ''Noise, chaos and (ϵ,τ)-entropy per unit time,'' Physics Reports **235**, 291–343 (1993).

[34] L. S. Tsimring, ''Nested strange attractors in spatiotemporal chaotic systems,'' Phys. Rev. E **48**, 3421–3426 (1993).

[35] C. Diks, J. C. van Houwelingen, F. Takens, and J. DeGoede, ''Reversibility as a criterion for discriminating time series,'' Phys. Lett. A **210**, 221–228 (1995).

[36] K. T. S. Konings, C. J. H. J. Kirchhof, J. R. L. M. Smeets, H. J. J. Wellens, O. C. Penn, and M. A. Allessie, ''High-density mapping of electrically induced atrial fibrillation in humans,'' Circulation **89**, 1665–1680 (1994).

[37] Y. A. Kuznetsov, *Elements of Applied Bifurcation Theory*, Springer Series in Applied Mathematical Sciences (Springer-Verlag, Berlin, 1994).

[38] G. K. Moe, ''On the multiple wavelet hypothesis of atrial fibrillation,'' Arch. Int. Pharmacodyn. Ther. **140**, 183–188 (1962).

[39] M. A. Allessie, W. J. E. P. Lammers, F. I. M. Bonke, and J. Hollen, ''Experimental evaluation of Moe's multiple wavelet hypothesis of atrial fibrillation,'' in *Cardiac Electrophysiology and Arrhythmias*, edited by D. P. Zipes and J. Jalife (Grune and Stratton, New York, 1985), pp. 265–275.

[40] J. L. Cox, T. E. Canavan, R. B. Schüssler, M. E. Cain, B. D. Lindsay, C. Stone, P. K. Smith, P. B. Corr, and J. P. Boineau, ''The surgical treatment of atrial fibrillation. II. Intraoperative electrophysiologic mapping and description of the electrophysiological basis of atrial flutter and atrial fibrillation,'' J. Thorac. Cardiovasc. Surg. **101**, 406–426 (1991).

[41] B. F. Hoffman and M. R. Rosen, ''Cellular mechanisms for cardiac arrhythmias,'' Circ. Res. **49**, 1–15 (1981).

[42] Z. Wang, P. Pagé, and S. Nattel, ''Mechanism of flecainide's antiarrhyth-

mic action in experimental atrial fibrillation,'' Circ. Res. **71**, 271–287 (1992).
[43] J. Wang, G. W. Bourne, Z. Wang, C. Villemaire, M. Talajic, and S. Nattel, ''Comparative mechanisms of antiarrhythmic drug action in experimental atrial fibrillation. Importance of use-dependent effects on refractoriness,'' Circulation **88**, 1030–1044 (1993).
[44] C. Kirchhof, M. Wijffels, J. Brugada, J. Planellas, and M. Allessie, ''Mode of action of a new class Ic drug (ORG 7797) against atrial fibrillation in conscious dogs,'' J. Cardiovasc. Pharmacol. **17**, 116–124 (1991).
[45] M. S. Spach and M. E. Josephson, ''Initiating reentry: The role of nonuniform anisotropy in small circuits,'' J. Cardiovasc. Electrophysiol. **5**, 182–209 (1994).
[46] A. S. Mikhailov and V. S. Zykov, ''Kinematical theory of spiral waves in excitable media: Comparison with numerical simulations,'' Physica D **52**, 379–397 (1991).
[47] A. S. Mikhailov, *Foundations of Synergetics I. Distributed Active Systems*, Springer Series in Synergetics (Springer-Verlag, Berlin, 1990).
[48] V. S. Zykov, *Simulation of Wave Processes in Excitable Media* (Manchester University Press, New York, 1987).
[49] R. A. Gray and J. Jalife, ''Spiral waves and the heart,'' Int. J. Bifurcation Chaos **6**, 415–435 (1996).
[50] A. T. Winfree, ''Varieties of spiral wave behavior: An experimentalist's approach to the theory of excitable media,'' Chaos **1**, 303–334 (1991).
[51] H. Tong, *Nonlinear Time Series Analysis: A Dynamical System Approach* (Oxford University Press, Oxford, 1990).
[52] D. A. Egolf and H. S. Greenside, ''Relation between fractal dimension and spatial correlation length for extensive chaos,'' Nature **369**, 129–131 (1994).
[53] C. D. Cutler and D. T. Kaplan, in *Nonlinear Dynamics and Time Series, Building a Bridge Between the Natural and Statistical Sciences*, Fields Institute Communications (American Mathematical Society, Providence, RI, 1997).
[54] P. Grassberger and I. Procaccia, ''Estimation of the Kolmogorov entropy from a chaotic signal,'' Phys. Rev. A **28**, 2591–2593 (1983).
[55] J. Theiler, ''Statistical precision of dimension estimators,'' Phys. Rev. A **41**, 3038–3051 (1990).
[56] J.-P. Eckmann and D. Ruelle, ''Fundamental limitations for estimating dimensions and Lyapunov exponents in dynamical systems,'' Physica D **56**, 185–187 (1992).
[57] C. Diks, W. R. van Zwet, F. Takens, and J. DeGoede, ''Detecting differences between delay vector distributions,'' Phys. Rev. E **53**, 2169–2176 (1996).